

Current Biology

Multi-scale goal distance representations in human hippocampus during virtual spatial navigation

Highlights

- Right hippocampal theta power decreases with goal proximity
- Goal distance modulation varies gradually along the hippocampal longitudinal axis
- Neural timescale shows a gradient decrease along the anterior-posterior hippocampus

Authors

Jiali Liu, Dong Chen, Xue Xiao, ...,
Andreas Schulze-Bonhage,
Nikolai Axmacher, Liang Wang

Correspondence

lwang@psych.ac.cn

In brief

Liu et al. examine goal distance representations in the hippocampus using the intracranial recordings in epilepsy patients. The results show that the theta-based goal distance modulation and neural timescales gradually change along the hippocampal longitudinal axis, indicating a coarse-to-fine goal distance representation in the human hippocampus.



Article

Multi-scale goal distance representations in human hippocampus during virtual spatial navigation

Jiali Liu,^{1,2,8} Dong Chen,^{1,2,8} Xue Xiao,^{1,2} Hui Zhang,³ Wenjing Zhou,⁴ Shuli Liang,⁵ Lukas Kunz,⁶ Andreas Schulze-Bonhage,⁷ Nikolai Axmacher,³ and Liang Wang^{1,2,9,*}

¹CAS Key Laboratory of Mental Health, Institute of Psychology, 16 Lincui Rd, Beijing 100101, China

²Department of Psychology, University of Chinese Academy of Sciences, 1 Yanqihu East Rd, Beijing 101408, China

³Department of Neuropsychology, Institute of Cognitive Neuroscience, Faculty of Psychology, Ruhr University Bochum, Universitätsstraße 150, Bochum 44801, Germany

⁴Department of Epilepsy Center, Tsinghua University Yuquan Hospital, 5 Shijingshan Rd, Beijing 100040, China

⁵Functional Neurosurgery Department, Beijing Children's Hospital, Capital Medical University, 56 Nanlishi Rd, Beijing 100045, China

⁶Department of Biomedical Engineering, Columbia University, 1210 Amsterdam Ave, New York, NY 10027, USA

⁷Epilepsy Center, Medical Center-University of Freiburg, Faculty of Medicine, University of Freiburg, Breisacher Str. 64, Freiburg im Breisgau 79106, Germany

⁸These authors contributed equally

⁹Lead contact

*Correspondence: lwang@psych.ac.cn

<https://doi.org/10.1016/j.cub.2023.04.033>

SUMMARY

Goal-directed navigation relies on both coarse and fine-grained coding of spatial distance between the current position of a navigating subject and a goal destination. However, the neural signatures underlying goal distance coding remain poorly understood. Using intracranial EEG recordings from the hippocampus of drug-resistant epilepsy patients who performed a virtual spatial navigation task, we found that the right hippocampal theta power was significantly modulated by goal distance and decreased with goal proximity. This modulation varied along the hippocampal longitudinal axis such that theta power in the posterior hippocampus decreased more strongly with goal proximity. Similarly, neural timescale, reflecting the duration across which information can be maintained, increased gradually from the posterior to anterior hippocampus. Taken together, this study provides empirical evidence for multi-scale spatial representations of goal distance in the human hippocampus and links the hippocampal processing of spatial information to its intrinsic temporal dynamics.

INTRODUCTION

Goal-directed navigation relies on multi-scale spatial coding of the distance between the current position and a goal destination.^{1–3} Imagine the scenario that you are traveling to a destination through a subway network. To navigate efficiently, you need not only to track gist information about the route (i.e., how often do I need to transfer between lines?), but also more fine-grained information (i.e., how many stations need to pass before transfer?). Multi-scale goal coding allows for efficient reorganization of spatial knowledge, is less susceptible to interference from background noise than coding at a single scale, and may support flexible navigation in environments with different sizes.^{1,4–8} However, the neural signatures underlying multi-scale goal coding remain poorly understood, particularly in the human brain.

Both animal and human studies have demonstrated that the hippocampus (HPC) plays fundamental roles in spatial goal coding.^{9–14} Functional magnetic resonance imaging (fMRI) studies have found that the HPC supports the prospective simulation of navigational events during planning¹⁵ and the hippocampal activity also encodes the distances to spatial goals during movement.^{9,11,16} Electrophysiological evidence has provided strong

support that hippocampal theta oscillations are associated with spatial navigation and episodic memory.¹⁷ In rodents, temporally compressed activations of place cells within theta cycles have been observed during movement, and some of these cells represent trajectories ahead of the animal.^{18,19} This phenomenon leads to the hypothesis that hippocampal theta oscillations may have critical roles in calculating future paths to remembered goals.²⁰ Furthermore, human intracranial electroencephalography (iEEG) studies showed that hippocampal theta oscillations is associated with distance processing.^{12,21} Therefore, it is reasonable to ask whether hippocampal theta oscillations are involved in the representation of goal distance.

In addition, human behavior experiments have shown that human can successfully navigate in the nested spatial environment, suggesting that our brains have a hierarchical representation of space.^{15,22,23} The fMRI studies also found that the HPC-prefrontal cortex hierarchically processes spatial information.^{1,3} Rodent studies showed that place field size increases gradually from dorsal to ventral HPC (homologous to the human posterior-anterior axis), putatively supporting a fine-to-coarse representation of the environment.^{2,24,25} Theoretical modeling shows that a fine-to-coarse representation is extremely efficient; by employing

Table 1. Demographic information

Recording site	Patient ID	Age (years)	Sex	R-HPC contacts	L-HPC contacts	R-Amyg contacts	Good trials	Bad trials
Beijing	1	25	M	0	4	0	77	14
Beijing	2	24	M	9	9	4	57	43
Beijing	3	23	M	7	0	5	32	83
Beijing	4	25	M	4	0	0	18	89
Beijing	5	31	F	4	5	4	21	60
Beijing	6	19	F	0	9	0	56	23
Freiburg	7	26	M	0	8	0	29	136
Beijing	8	27	M	0	9	0	44	65
Beijing	9	36	F	13	0	0	16	38
Freiburg	10	34	M	3	0	2	67	62
Beijing	11	24	M	4	2	4	26	70
Beijing	12	28	M	4	0	2	18	34
Beijing	13	32	M	0	6	0	16	20
Beijing	14	22	M	11	0	4	58	49
Beijing	15	19	F	0	10	0	20	44

M, male; F, female; R, right; L, left; HPC, hippocampus; Amyg, amygdala.

neurons with different place field size, the overall spatial resolution scales exponentially with the number of neurons.⁸ To achieve it, more cells with smaller place fields are needed than cells with larger place field.⁵ We therefore hypothesized that during goal tracking, the posterior HPC may recruit more cells, resulting in a gradient in the representation of the HPC to goal distance coding.

To track goal distances at a fine-grained scale, the relevant brain areas must activate transiently to couple rapidly changing external stimuli.²⁶ In contrast, coding goal distances at a coarse-grained scale, the relevant brain areas must activate persistently to integrate more information.^{26,27} Thus the spatial organization hierarchy for goal location processing needs to be converted to the time domain.^{27,28} The temporal hierarchy can be measured by the so-called neural timescale, which reflects how long a local network can be persistently active²⁹ and is largely determined by intrinsic dynamic properties.²⁷ We estimated the neural timescale for each hippocampal contact during the navigation task, and tested the hypothesis that neural timescales exhibit gradients along the hippocampal axis, attempting to link the hippocampal processing of spatial information to its temporal dynamics and reveal the neural computational mechanism of gradient representation of spatial information.

To test these predictions, we examined intracranial recordings of hippocampal activity in drug-resistant epilepsy patients who performed an object-location memory task. We found that theta power was significantly modulated by goal distance, with decreasing power closer to the goal. Importantly, this modulation changed gradually along the hippocampal longitudinal axis, such that theta power in the posterior HPC decreased more strongly with goal proximity. We furthermore found that the neural timescales showed a similar gradual increase from posterior to anterior HPC. Our results provided empirical evidence for a fine-to-coarse representation of spatial-temporal information in human HPC.

RESULTS

Right hippocampal theta oscillations predict goal distance

Participants performed a self-paced navigation task on the laptop while intracranial EEG data were recorded (Table 1). In this task, they first collected eight everyday objects placed in different locations one after the other, then continuously performed memory recall tests (Figure 1A). Participants freely navigated to the remembered location of the cued object and indicated this location with a button press. This was followed by feedback (via smileys of different colors depending on accuracy) and presentation of the target object at its correct location, from where participants recollected the object. We characterized the normalized power spectrum in all hippocampal contacts during fast movement in the retrieval phases. We observed two peaks centered around ~2 and 7 Hz, respectively (Figure 2B), and high theta power (6–9 Hz) during fast retrieval epochs (defined as periods with exceeding the fastest tercile of all movement speed during retrieval phases) were significantly higher than average high theta power of all movement ($t(120) = 2.331$, $p = 0.021$; Figure 2C), consistent with previous studies.^{21,30,31}

We characterized the relationship between high theta power and goal distance (defined as the Euclidean distance between the instantaneous location and the true goal location) in the left and right HPC, respectively, since previous studies proposed that lateralized hippocampal oscillations might underlie distinct aspects of human cognition, with right hippocampal theta oscillations being more engaged in spatial navigation.³¹ In line with our hypotheses, we found that right hippocampal theta power was significantly modulated by goal distance (Figure 2D), with theta power being higher when participants were further away from the goal (Figures 2E and 2F). This modulation was behaviorally relevant, since it only existed in trials with good performance ($t(58) = 3.063$, $p = 0.003$), but not in trials with bad performance ($t(58) = -0.983$, $p = 0.330$). Theta power in right HPC was also

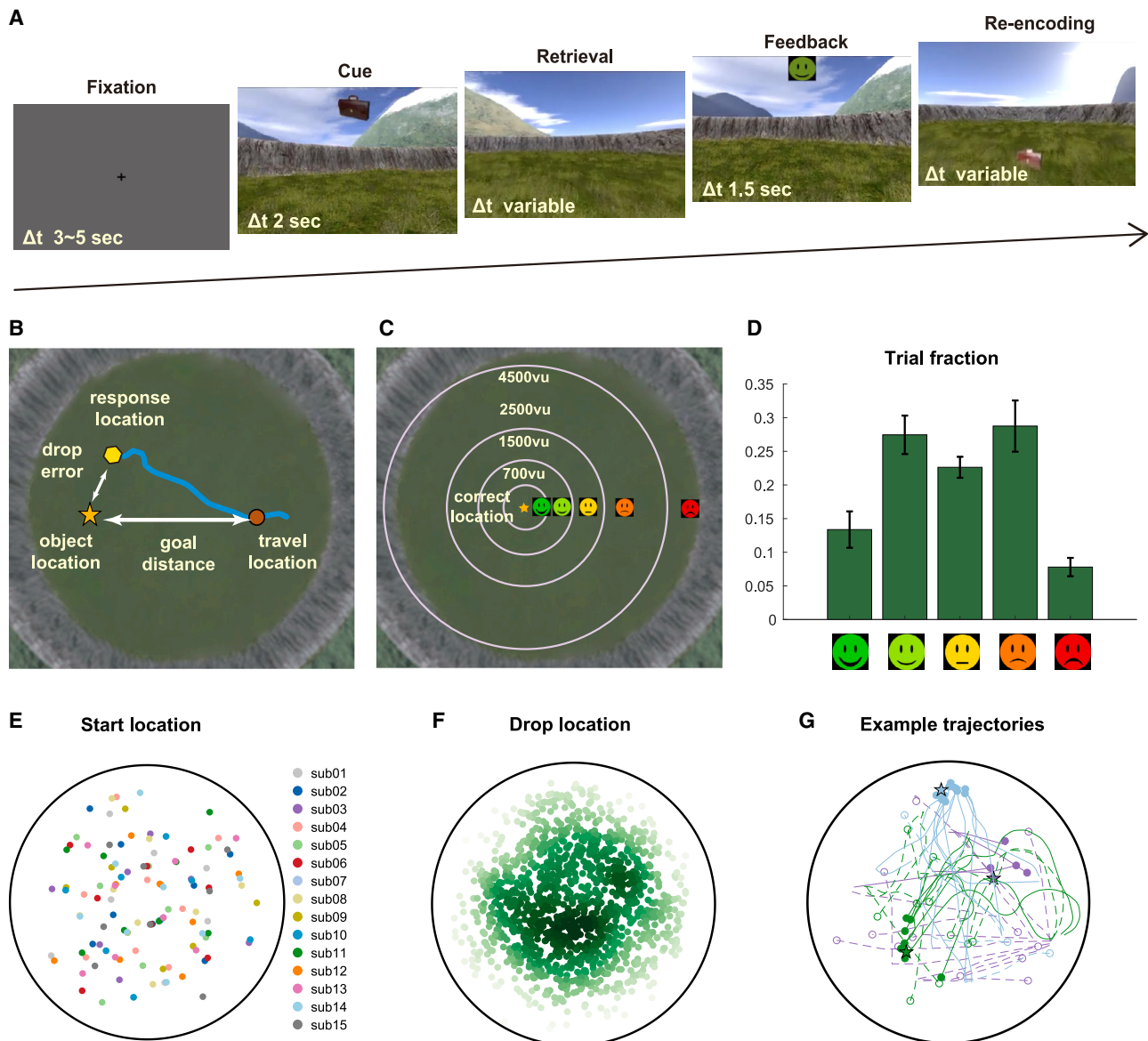


Figure 1. Experimental paradigm and behavioral results

(A) Object location memory task.

(B) Drop error was defined as the Euclidean distance between the response location (yellow hexagon) and the actual object location (orange pentagram). Goal distance was calculated as the instantaneous Euclidean distance between the current location (brown circle) and the correct object location. The blue curve is an example of movement trajectory.

(C) Feedback to participants depended on drop error. We divided the trials into two categories: good trials (dark and light green smileys) and bad trials (yellow, dark red, and light red expressions).

(D) Fraction of trials with different types of feedback, i.e., different drop errors ($n = 15$ participants).

(E) All start locations.

(F) All termination locations. The color represents the density, the darker the higher the density.

(G) Example trajectories: all trajectories to a particular goal in 3 subjects (different color) for good (solid lines and solid circles) and bad trials (dotted lines and hollow circles). The pentagram marks the target location, while the circle marks the response location.

See also Figure S5.

significantly modulated by subjective goal distance (i.e., the Euclidean distance between the subject's current location and their response location) in good trials ($t(58) = 2.018$, $p = 0.048$; Figure S1A), but not in bad trial ($t(58) = -0.926$, $p = 0.358$; Figure S1A). As expected, the modulation of subjective goal

distance in the right HPC showed a significant correlation with the modulation of objective goal distance (same as goal distance) in good trials ($p < 0.001$; Figure S1B). In contrast, we did not observe an effect of goal distance on theta power in the left HPC for either good trials ($t(61) = -0.791$, $p = 0.432$;

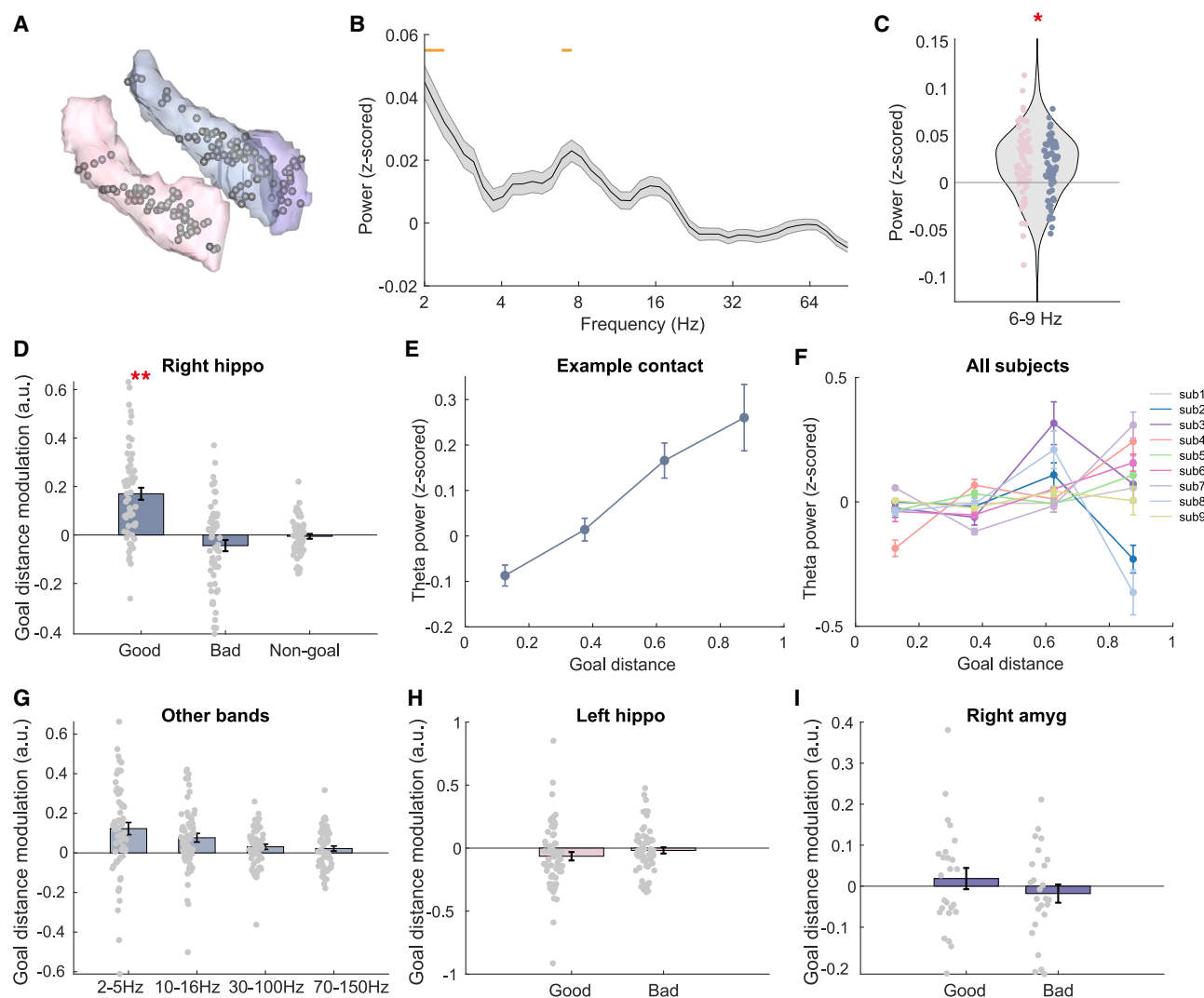


Figure 2. Theta-based goal distance modulation in the right hippocampus

(A) All electrode contacts (gray circles) in the right hippocampus (blue), left hippocampus (pink), and right amygdala (purple). (B) Power spectrum of the hippocampus showed a peak frequency between 6 and 9 Hz during fast movement periods of memory retrieval. (C) Normalized theta power (6–9 Hz) during fast movement periods of memory retrieval was significantly higher than zero. The pink and blue dots refer to the normalized theta power for left and right hippocampal contacts respectively. (D) Significant correlation between right hippocampal theta power and goal distance in good trials, but not in bad trials and for non-target goals. Goal distance refers to instantaneous Euclidean distance between the current location and the correct object location. (E) Example contact in the right hippocampus showing a positive correlation between theta power and goal distance. (F) Normalized right hippocampal theta power is depicted as a function of goal distance quartiles for each subject. (G) Low theta (2–5 Hz), alpha/beta (10–16 Hz), gamma (30–100 Hz), and high gamma (70–150 Hz) power in the right hippocampus were not modulated by goal distance. (H and I) Goal distance modulation was not significant in the left hippocampus (H) and right amygdala (I). * $p < 0.05$, ** $p < 0.01$. Yellow bars represent significant frequency bins. See also [Figures S1–S3](#).

Figure 2H) or bad trials ($t(61) = -0.289$, $p = 0.774$), and no effect of subjective goal distance ($t(61) = -0.841$, $p = 0.404$; [Figure S1A](#)), although there was no difference in high theta power between the left and right HPC ($t(119) = -1.608$, $p = 0.111$).

We conducted a series of control analyses. To exclude the possibility that different goal distance modulation in good and bad trials was attributed to differences in theta power, right hippocampal theta power of the two condition was compared and no

significant difference appeared ($t(58) = -0.821$, $p = 0.415$). To ensure that theta activity was indeed modulated by the distance to the actual target in a given trial, we correlated theta power with the Euclidean distance to a randomly selected non-target goal. Results showed that theta power was not modulated by non-target distance ($t(58) = -0.272$, $p = 0.786$; [Figure 2D](#)). We also repeated the analysis of goal distance for contacts in the right amygdala, close to the right HPC. We did not find an effect of goal

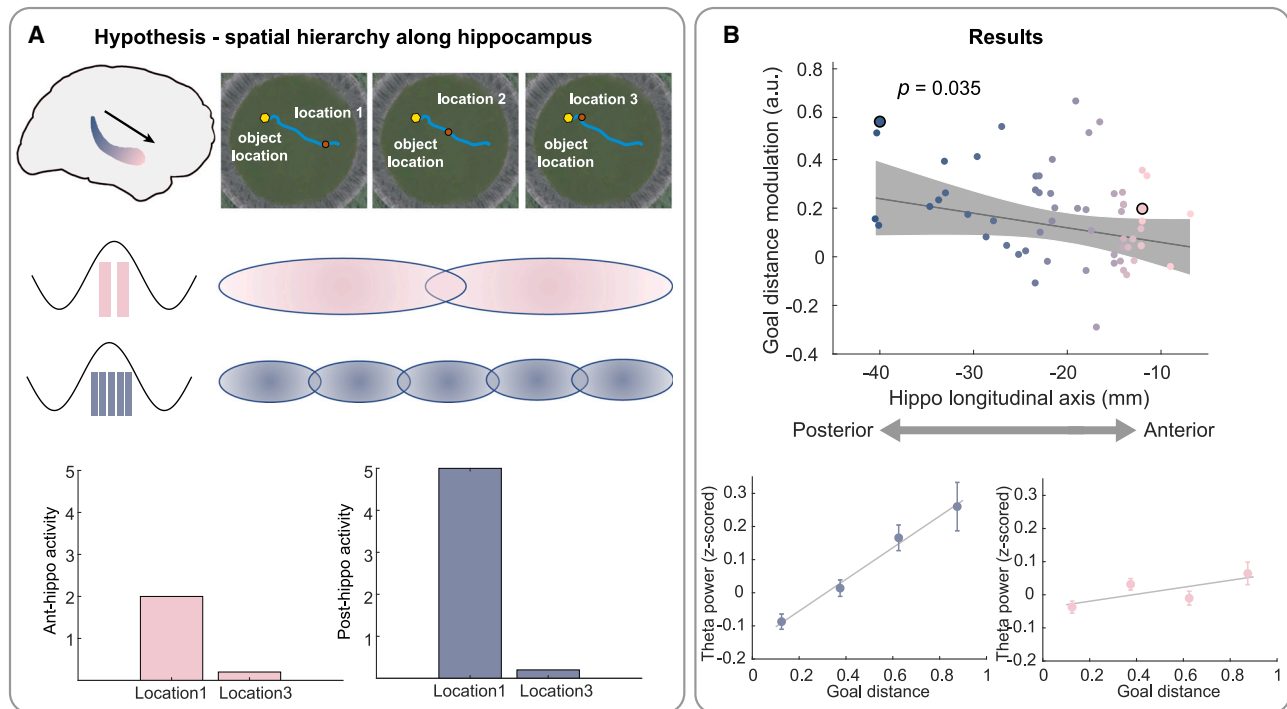


Figure 3. A gradient of goal distance modulation along the hippocampal longitudinal axis

(A) Schematic depiction of hypothesized multi-scale goal distance representations along the hippocampal longitudinal axis. Previous electrophysiological recordings showed gradually increasing place field sizes along the posterior-anterior axis (illustrated by the black arrow, top). While traveling to the goal, place cells are organized by the theta oscillation (middle). Due to smaller place field sizes in the posterior hippocampal neurons, more cells are recruited during longer trajectories, and stronger theta oscillations may be required to organize these place cells. Theta activities in the posterior hippocampus may thus change more rapidly when a goal destination is approached (bottom).

(B) Goal distance modulation correlates with recording locations along the right hippocampal posterior-anterior axis (top). As examples (bottom), the goal distance is plotted against theta power for the circled blue and pink dots marked at the top panel.

See also Figure S4.

distance modulation in either good trials ($t(24) = 0.281$, $p = 0.781$; Figure 2I) or bad trials ($t(24) = -0.203$, $p = 0.841$). No goal distance modulation was observed in other frequency bands in the right HPC (2–5 Hz: $t(58) = 1.758$, $p = 0.084$; 10–16 Hz: $t(58) = 1.459$, $p = 0.150$; 30–100 Hz: $t(58) = 1.026$, $p = 0.309$; 70–150 Hz: $t(58) = 0.519$, $p = 0.606$; Figure 2G). Given the fact that goal distance was related to traveled time (Figure S5), we furthermore regressed the elapsed time with theta power, but did not find a significant effect for either good trials ($t(58) = 1.061$, $p = 0.293$; Figure S2D) or bad trials ($t(58) = 1.380$, $p = 0.173$). Both path distance to goal and Euclidean goal distance are vital variables in goal-directed navigation.¹¹ We thus correlated path distance to goal with theta power, but did not find a significant effect for either good trials ($t(58) = 1.086$, $p = 0.282$; Figure S2A) or bad trials ($t(58) = -0.289$, $p = 0.774$). During navigation in the open arena, sometimes the trajectory was not straight (e.g., the green curves in Figure 1G), which can make the path distance be different from the Euclidean distance to the goal. Finally, some research suggested that the HPC is involved in egocentric direction coding.^{11,14} We thus used goal distance, egocentric direction, and the interaction between goal distance and egocentric direction as regressors in good trials. Theta power was not related to egocentric direction ($t(58) = 0.421$, $p = 0.675$; Figure S3B) and the interaction ($t(58) = -0.995$, $p = 0.324$).

Confounding factors such as boundary and speed cannot explain the results of goal modulation

Previous studies have reported that theta oscillations in the HPC are related to spatial variables such as boundaries and speed.^{30,32,33} We analyzed the impact of these potential confounding factors. We thus correlated the boundary distance (distance between the subject's current position and the boundary) with theta power in good trials. The result showed that the modulation of high theta power (6–9 Hz) by the boundary was not significant ($t(58) = -0.697$, $p = 0.489$; Figure S3A). However, we did find that low theta power was modulated by the boundary; it increased as subjects approached the boundary, consistent with a previous study ($t(58) = -2.182$, $p = 0.033$; Figure S3A).³² Furthermore, after controlling for boundary distance, we found that the high theta power was still significantly modulated by the goal distance ($t(58) = 2.550$, $p = 0.013$). Intuitively, when the goal was closer to the boundary, subjects may tend to use it to extract location information for goal distance calculation. Therefore, we examined the effect of distance between the goal location and the boundary. We found that theta power was still significantly modulated by the goal distance ($t(58) = 2.229$, $p = 0.030$), but not by the distance of the goal to the boundary ($t(58) = 1.689$, $p = 0.097$). The two terms did not show an interaction ($t(58) = -0.992$, $p = 0.325$).

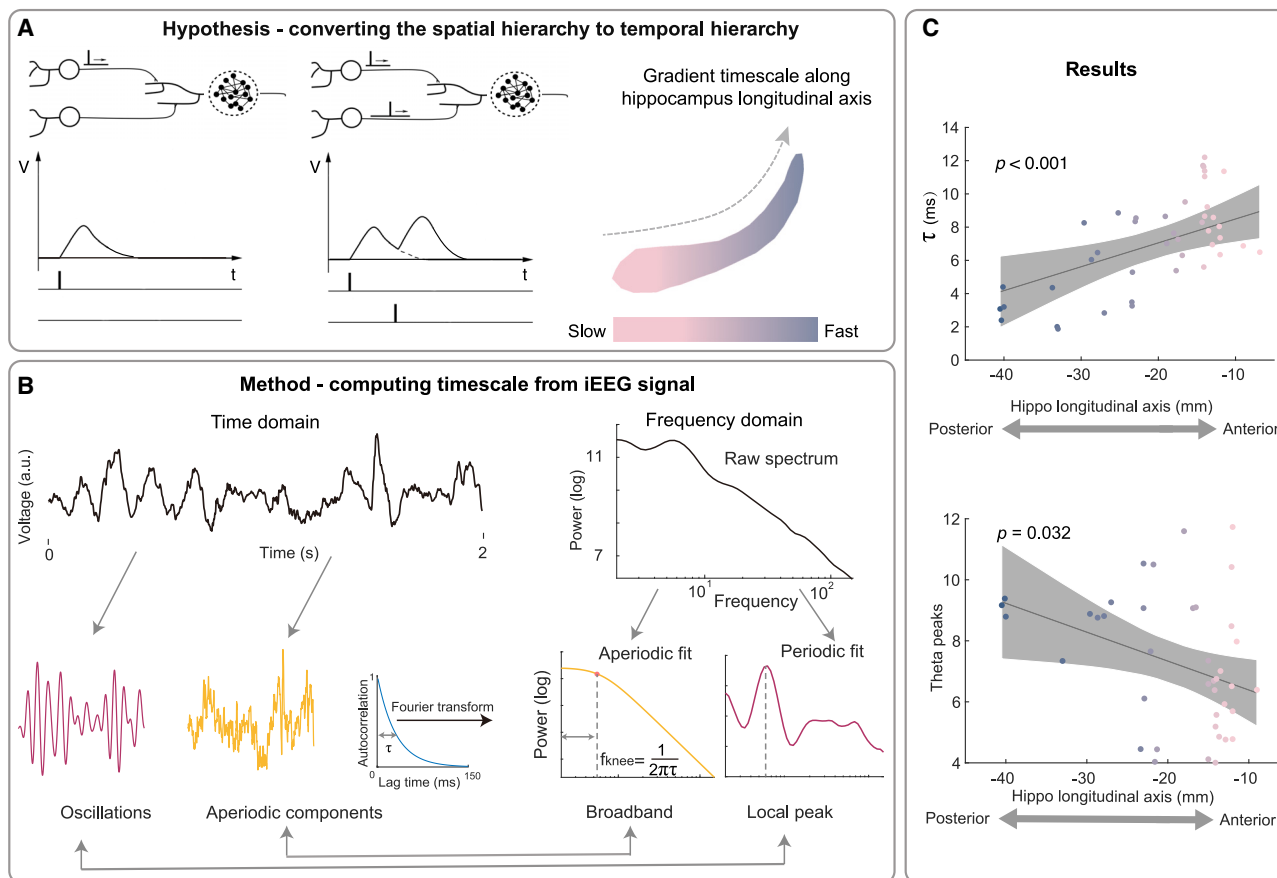


Figure 4. Temporal hierarchies increase gradually along the hippocampal longitudinal axis

(A) The concept of neural timescale and hypothesis. Neural timescale can be defined as the decay speed of neural signals, reflecting the ability to integrate information. Only when the interval between the two upstream signals is shorter than the timescale, the downstream network can integrate the two information. We exhibit our hypothesis—the hippocampal axis may have a gradient of timescale.

(B) Two complementary methods for computing temporal hierarchies from neural signals: broadband feature (neural timescale, i.e., τ) and local peaks from power spectrum density, corresponding to aperiodic and periodic components.

(C) The relationship between neural timescale (or theta peak) and position along the hippocampal longitudinal axis. There is a significant gradient of τ (top) and theta peak (bottom) along the hippocampal anterior-posterior axis.

In addition, we also considered possible influences of speed and acceleration. First, we used the same method to analyze the modulation of theta power with goal distance during medium-speed and low-speed epochs, and the results were not significant (low speed: $t(58) = 1.068$, $p = 0.290$; medium speed: $t(58) = 1.412$, $p = 0.163$; Figure S3C). These results are similar to previous work, including ours, that is, in virtual navigation, the processing of spatial information is more pronounced in high-speed epochs, which may be related to a stronger sense of involvement of the subjects.^{34–36} We note that the instantaneous speed of participants was changing even in the high-speed movement epochs. We thus added the instantaneous speed and the acceleration/deceleration into the regression equation, respectively. However, none of these potentially confounding factors affected the modulation of the goal distance (speed: $t(58) = 3.099$, $p = 0.003$; acceleration: $t(58) = 2.489$, $p = 0.016$; deceleration: $t(58) = 2.283$, $p = 0.026$), and these covariates themselves were not significant (speed: $t(58) = 1.343$, $p = 0.185$;

acceleration: $t(58) = -0.326$, $p = 0.746$; deceleration: $t(58) = 0.063$, $p = 0.950$).

Effect of goal distance on theta power varies along the longitudinal axis of the HPC

The size of rodent place fields increases gradually along the dorsal-to-ventral axis of the HPC (homologous to the human posterior-anterior axis), reflecting a hierarchy of spatial representations.²⁵ We hypothesized that goal distance coding may vary gradually along the human hippocampal axis as well. We examined the relationship between goal distance modulation (i.e., β values) and the y axis coordinates of the recording sites in the HPC. As expected, goal distance modulation in good trials showed a gradient along the right hippocampal longitudinal axis: Theta power changed with goal distance more rapidly (i.e., higher β values) in the posterior HPC and more slowly (i.e., lower β values) in the anterior HPC, indicating a coarse-to-fine coding of goal distance across multiple spatial scales ($t(57) = -2.160$, $p = 0.035$; Figure 3B). When controlling for theta

power, the correlation between goal distance modulation and position along the hippocampal longitudinal axis was still significant ($t(56) = -2.230$, $p = 0.029$). In contrast, the goal distance modulation in bad trials did not show such a gradient ($t(57) = 0.378$, $p = 0.707$; Figure S4C), and no gradient was observed along the longitudinal axis of the left hippocampal in either good ($t(60) = 0.076$, $p = 0.940$; Figure S4A) or bad trials ($t(60) = -1.543$, $p = 0.128$; Figure S4B).

Transfer of spatial hierarchy to temporal hierarchy along the hippocampal longitudinal axis

Neural timescale can be defined as how long a local network can be persistently active.²⁶ This feature reflects the ability to integrate information, and is determined by the area's intrinsic dynamic properties.²⁷ At the single neuron level, roughly speaking, the magnitude of the neural timescale is similar to the membrane time constant, which is the duration for neurons to return from action potential to resting potential. If the interval between the two spike signals A and B in the upstream is greater than this duration, then the downstream neuron C cannot integrate the information, because the membrane potential pushed up by A has returned to baseline before B arrives (Figure 4A). At the scale of neural assemblies, the timescale can be measured from local field potential (LFP) data.^{26,37} Above results showed that anterior HPC tracked goal distances at a coarse-grained scale, suggesting a role in integrating more information. We hypothesize that it should have a larger timescale, occupying a higher temporal hierarchy.

Here, we estimated the neural timescale with recent well-development method, which concerns the non-periodic component of LFP signal.²⁶ In this way, neural timescale can be calculated by the knee frequency in the broadband part of the spectrum, using the formula $\tau = \frac{1,000}{2\pi f_{knee}}$ (Figure 4B). The result showed a gradually increasing timescale from posterior to anterior HPC ($t(40) = 4.667$, $p < 0.001$; Figure 4C upper part). The correlation between τ and goal distance modulation was negative as expected, although only marginally significant ($t(40) = -1.706$, $p = 0.096$). Local peak of the spectrum, the periodic component of the LFP signal, is another complementary measure to reflect temporal hierarchy. We speculated that the posterior HPC shows higher frequency theta oscillations, thus changing faster. Similarly, we found a gradually increasing theta peak frequency along the longitudinal axis ($t(38) = -2.230$, $p = 0.032$; Figure 4C lower part), consistent with the previous study.³⁰ The correlation between goal distance modulation and theta peak frequency was not significant ($t(38) = 1.256$, $p = 0.217$). These results indicate a transfer of spatial hierarchy to temporal hierarchy along the hippocampal longitudinal axis.

DISCUSSION

This study examined how the HPC dynamically encodes goal distance during virtual navigation. We found that theta power (6–9 Hz) in the right HPC was positively related to Euclidean goal distance. Critically, goal distance modulation changed gradually along the hippocampal longitudinal axis, with stronger correlations between goal distance and theta power in posterior

than anterior HPC. We also found that neural timescales in posterior HPC were faster than in anterior HPC. These results suggest that the HPC exhibits spatiotemporal representations at multiple scales, which may be critical to guide flexible and precise navigation to goal destinations.

Previous human fMRI studies yielded contradictory results about hippocampal coding of goal distance. Some studies showed increased hippocampal activities with goal distance,^{9,11} whereas others showed the reverse effect.^{1,38,39} It was suggested that the influence of goal distances on hippocampal activity depends on the size of navigational environments: in larger spaces, hippocampal activity showed a positive correlation,^{11,40} while this effect reversed in smaller and more constrained environments.^{1,38,39} A recent study reported that navigation phase also plays a role. Specifically, HPC activity increased with goal distance during travel, but decreased at decision points.¹¹ Another study found that environmental complexity not only affected navigational behavior but also modulated HPC activity, with greater hippocampal activity in simpler environments.⁴¹ In the current study, we found positive correlations between hippocampal theta power and goal distance. However, due to complex relationships between theta power and fMRI BOLD signals in the HPC,^{42,43} our results cannot be directly compared with the fMRI studies mentioned above.

We found hippocampal theta power to be positively modulated by goal distance. Consistent with our results, a rodent study found that Cornu Ammonis 1 region (CA1) activity was positively correlated with goal distance, which means CA1 activity decreases with proximity to the goal.⁴⁴ Furthermore, the stronger the correlation was, the better the behavioral performance. This is also consistent with our findings since we only found goal distance modulation of theta power in good trials. We speculate that when more cells are recruited during longer trajectories, more pronounced theta oscillations may be required to organize these place cells, leading to a positive correlation between goal distance and theta power. Align with our speculation, recent studies have shown that theta oscillations in the HPC plays an extremely important role in organizing the sequential discharge of place cells: the excitation-inhibition time window created by theta can regulate spike timing of place cells.^{17,28,45} A recent study found that after injecting muscimol to perturb the internal theta oscillation, it was the fire sequence but not fire rate of place cell being affected.⁴⁵ However future studies are needed to exclude the possibility that the increased theta oscillations away from the goal is a side effect of more cells firing synchronously.

The current study showed that Euclidean goal distances were associated with theta power in the right HPC, but not in the left HPC, providing evidence for a lateralization of hippocampal functions. Consistent with our results, previous fMRI studies found that only right hippocampal activity was modulated by goal distance during traveling.^{9,11} In addition, a human intracranial EEG study found different cognitive functions supported by left and right HPC, showing that the left HPC was relevant for successful memory encoding, while the right HPC was recruited during spatial navigation.³¹ Lateralized functions in the HPC were also associated with navigational strategies, with sequential egocentric representations in the left HPC and allocentric representations in the right HPC.⁴⁶ The current study involves

navigation in an open maze, which may rely more on an allocentric strategy and thus the right HPC.

Our results found that a posterior-to-anterior gradient of neural timescales along the hippocampal axis. The longer neural timescale in the anterior HPC might underlying the neural mechanism the distribution of rodent place field sizes. Neurons in anterior HPC have greater neural timescales and could activate for a longer period, thus show larger place fields when rodents cross the environment. Furthermore, the gradient of neural timescales might also underlie the goal distance coding. Neurons with shorter timescales in the posterior HPC are more tightly coupled to rapid changes in the external environment, consistent with our finding that theta power in the right posterior HPC is coupled more tightly to goal distance. Combined with a series of previous studies, these results suggest a coarse-to-fine representation along the hippocampal longitudinal axis.^{2,3} However, recent rodent study found that not only the fields of ventral (anterior equivalent) hippocampal cells do extend, but also the stability and spatial selectivity of the place cells decreased.⁴⁷ This result implies another account: gradient changes of spatial representation from posterior to anterior HPC may reflect a reduction of spatial coding, as opposed to a shift to large-scale coding. Future studies are warranted to distinguish these two possibilities.

Neural representations of goal distance may differ between open mazes without any obstacles and city environments with many buildings. First, in structured city environments, one may not calculate goal distance at every time point, for example, when coasting along a pedestrian bridge.^{48,49} By contrast, in open maze environments with only distal cues, calculating the goal distance at every time point may be required to accurately reach a goal. Second, it is worth noting that both path distance and Euclidean goal distance are vital variables. The representation of path distance to a goal is critical for selecting optimal routes and avoiding dead ends, whereas the representation of Euclidean goal distances allows to select shortcuts. However, detours only exist in structured (e.g., city) environments, but not in open maze environments. Therefore, continuously tracking Euclidean goal distance may be more critical in our task than tracking path distance. A previous fMRI study on navigation in a city environment found that the posterior HPC was sensitive to the path distance to goals, while activity in anterior HPC was correlated with the Euclidean distance to a goal.¹¹ In the current study with an open maze environment, we found hippocampal theta power to be only correlated with Euclidean goal distance. This controversy might result from the environment and task demand.

Overall, by examining direct intracranial recordings of hippocampal activity, this study found that high theta power (6–9 Hz) dynamically tracked goal distance and decreased when participants approached the goal. Critically, both goal distance modulation and neural timescales consistently showed gradual changes along the hippocampal longitudinal axis. These results provide empirical evidence for a multi-scale spatiotemporal representation in the human HPC.

STAR★METHODS

Detailed methods are provided in the online version of this paper and include the following:

- **KEY RESOURCES TABLE**
- **RESOURCE AVAILABILITY**
 - Lead contact
 - Materials availability
 - Data and code availability
- **EXPERIMENTAL MODEL AND STUDY PARTICIPANT DETAILS**
- **METHOD DETAILS**
 - Experiment task
 - Intracranial EEG recordings and preprocessing
 - Electrode localization
 - Data analysis
- **QUANTIFICATION AND STATISTICAL ANALYSIS**

SUPPLEMENTAL INFORMATION

Supplemental information can be found online at <https://doi.org/10.1016/j.cub.2023.04.033>.

ACKNOWLEDGMENTS

We are grateful to the patients for participating in our study. This study was supported by the STI2030-Major Projects (2022ZD0205000), the National Natural Science Foundation of China (32020103009), the Ministry Key Project (GW0890006), the CAS Interdisciplinary Innovation Team (JCTD-2018-07), and the Scientific Foundation of the Institute of Psychology, Chinese Academy of Sciences (E2CX4215CX). N.A. received support via funding from the ERC grant agreement (864164) (ERC-CoG “GridRepresentations”). D.C. was supported by the National Natural Science Foundation of China (32200861), China Postdoctoral Science Foundation (2019M660850), and CAS Special Research Assistant Project.

AUTHOR CONTRIBUTIONS

Conceptualization, L.W.; investigation, D.C., H.Z., W.Z., S.L., L.K., and A.S.-B.; formal analysis, J.L., D.C., and X.X.; supervision, L.W.; writing – original draft, J.L.; writing – review & editing, J.L., D.C., N.A., and L.W.

DECLARATION OF INTERESTS

The authors declare no competing interests.

INCLUSION AND DIVERSITY

We support inclusive, diverse, and equitable conduct of research.

Received: December 29, 2022

Revised: March 17, 2023

Accepted: April 14, 2023

Published: May 5, 2023

REFERENCES

1. Balaguer, J., Spiers, H., Hassabis, D., and Summerfield, C. (2016). Neural mechanisms of hierarchical planning in a virtual subway network. *Neuron* 90, 893–903.
2. Brunec, I.K., Bellana, B., Ozubko, J.D., Man, V., Robin, J., Liu, Z.-X., Grady, C., Rosenbaum, R.S., Winocur, G., and Barense, M.D. (2018). Multiple scales of representation along the hippocampal anteroposterior axis in humans. *Curr. Biol.* 28, 2129–2135.e6.
3. Brunec, I.K., and Momennejad, I. (2022). Predictive representations in hippocampal and prefrontal hierarchies. *J. Neurosci.* 42, 299–312. <https://doi.org/10.1523/JNEUROSCI.1327-21.2021>.

4. Raut, R.V., Snyder, A.Z., and Raichle, M.E. (2020). Hierarchical dynamics as a macroscopic organizing principle of the human brain. *Proc. Natl. Acad. Sci. USA* 117, 20890–20897.
5. Zhang, H., Rich, P.D., Lee, A.K., and Sharpee, T.O. (2023). Hippocampal spatial representations exhibit a hyperbolic geometry that expands with experience. *Nat. Neurosci.* 26, 131–139. <https://doi.org/10.1038/s41593-022-01212-4>.
6. Zhang, K., and Sejnowski, T.J. (1999). Neuronal tuning: to sharpen or broaden? *Neural Comput.* 11, 75–84. <https://doi.org/10.1162/089976699300016809>.
7. Kriegeskorte, N., and Wei, X.-X. (2021). Neural tuning and representational geometry. *Nat. Rev. Neurosci.* 22, 703–718. <https://doi.org/10.1038/s41583-021-00502-3>.
8. Mathis, A., Herz, A.V., and Stemmler, M.B. (2012). Resolution of nested neuronal representations can be exponential in the number of neurons. *Phys. Rev. Lett.* 109, 018103. <https://doi.org/10.1103/PhysRevLett.109.018103>.
9. Spiers, H.J., and Maguire, E.A. (2007). A navigational guidance system in the human brain. *Hippocampus* 17, 618–626. <https://doi.org/10.1002/hipo.20298>.
10. Nyberg, N., Duvelle, É., Barry, C., and Spiers, H.J. (2022). Spatial goal coding in the hippocampal formation. *Neuron* 110, 394–422.
11. Howard, L.R., Javadi, A.H., Yu, Y., Mill, R.D., Morrison, L.C., Knight, R., Loftus, M.M., Staskute, L., and Spiers, H.J. (2014). The hippocampus and entorhinal cortex encode the path and Euclidean distances to goals during navigation. *Curr. Biol.* 24, 1331–1340.
12. Vass, L.K., Copara, M.S., Seyal, M., Shahlaie, K., Farias, S.T., Shen, P.Y., and Ekstrom, A.D. (2016). Oscillations go the distance: low-frequency human hippocampal oscillations code spatial distance in the absence of sensory cues during teleportation. *Neuron* 89, 1180–1186. <https://doi.org/10.1016/j.neuron.2016.01.045>.
13. Pfeiffer, B.E., and Foster, D.J. (2013). Hippocampal place-cell sequences depict future paths to remembered goals. *Nature* 497, 74–79.
14. Sarel, A., Finkelstein, A., Las, L., and Ulanovsky, N. (2017). Vectorial representation of spatial goals in the hippocampus of bats. *Science* 355, 176–180.
15. Brown, T.I., Carr, V.A., LaRocque, K.F., Favila, S.E., Gordon, A.M., Bowles, B., Bailenson, J.N., and Wagner, A.D. (2016). Prospective representation of navigational goals in the human hippocampus. *Science* 352, 1323–1326. <https://doi.org/10.1126/science.aaf0784>.
16. Bierbrauer, A., Kunz, L., Gomes, C.A., Luhmann, M., Deuker, L., Getzmann, S., Wascher, E., Gajewski, P.D., Hengstler, J.G., Fernandez-Alvarez, M., et al. (2020). Unmasking selective path integration deficits in Alzheimer's disease risk carriers. *Sci. Adv.* 6, eaba1394.
17. Herweg, N.A., Solomon, E.A., and Kahana, M.J. (2020). Theta oscillations in human memory. *Trends Cogn. Sci.* 24, 208–227.
18. Dragoi, G., and Buzsáki, G. (2006). Temporal encoding of place sequences by hippocampal cell assemblies. *Neuron* 50, 145–157.
19. Foster, D.J., and Wilson, M.A. (2007). Hippocampal theta sequences. *Hippocampus* 17, 1093–1099.
20. Wikenheiser, A.M., and Redish, A.D. (2015). Hippocampal theta sequences reflect current goals. *Nat. Neurosci.* 18, 289–294.
21. Bush, D., Bisby, J.A., Bird, C.M., Gollwitzer, S., Rodionov, R., Diehl, B., McEvoy, A.W., Walker, M.C., and Burgess, N. (2017). Human hippocampal theta power indicates movement onset and distance travelled. *Proc. Natl. Acad. Sci. USA* 114, 12297–12302. <https://doi.org/10.1073/pnas.1708716114>.
22. Wang, R.F., and Brockmole, J.R. (2003). Simultaneous spatial updating in nested environments. *Psychon. Bull. Rev.* 10, 981–986. <https://doi.org/10.3758/BF03196562>.
23. Wang, R.F., and Brockmole, J.R. (2003). Human navigation in nested environments. *J. Exp. Psychol. Learn. Mem. Cogn.* 29, 398–404. <https://doi.org/10.1037/0278-7393.29.3.398>.
24. Kjelstrup, K.B., Solstad, T., Brun, V.H., Hafting, T., Leutgeb, S., Witter, M.P., Moser, E.I., and Moser, M.-B. (2008). Finite scale of spatial representation in the hippocampus. *Science* 321, 140–143.
25. Strange, B.A., Witter, M.P., Lein, E.S., and Moser, E.I. (2014). Functional organization of the hippocampal longitudinal axis. *Nat. Rev. Neurosci.* 15, 655–669.
26. Gao, R., van den Brink, R.L., Pfeffer, T., and Voytek, B. (2020). Neuronal timescales are functionally dynamic and shaped by cortical microarchitecture. *eLife* 9, e61277.
27. Chaudhuri, R., Knoblauch, K., Gariel, M.-A., Kennedy, H., and Wang, X.-J. (2015). A large-scale circuit mechanism for hierarchical dynamical processing in the primate cortex. *Neuron* 88, 419–431.
28. Buzsáki, G., and Tingley, D. (2018). Space and time: the hippocampus as a sequence generator. *Trends Cogn. Sci.* 22, 853–869. <https://doi.org/10.1016/j.tics.2018.07.006>.
29. Duarte, R., Seeholzer, A., Zilles, K., and Morrison, A. (2017). Synaptic patterning and the timescales of cortical dynamics. *Curr. Opin. Neurobiol.* 43, 156–165.
30. Goyal, A., Miller, J., Qasim, S.E., Watrous, A.J., Zhang, H., Stein, J.M., Inman, C.S., Gross, R.E., Willie, J.T., Lega, B., et al. (2020). Functionally distinct high and low theta oscillations in the human hippocampus. *Nat. Commun.* 11, 2469. <https://doi.org/10.1038/s41467-020-15670-6>.
31. Miller, J., Watrous, A.J., Tsitsiklis, M., Lee, S.A., Sheth, S.A., Schevon, C.A., Smith, E.H., Sperling, M.R., Sharan, A., and Asadi-Pooya, A.A. (2018). Lateralized hippocampal oscillations underlie distinct aspects of human spatial memory and navigation. *Nat. Commun.* 9, 1–12.
32. Stangl, M., Topalovic, U., Inman, C.S., Hiller, S., Villaroman, D., Aghajan, Z.M., Christov-Moore, L., Hasulak, N.R., Rao, V.R., Halpern, C.H., et al. (2021). Boundary-anchored neural mechanisms of location-encoding for self and others. *Nature* 589, 420–425. <https://doi.org/10.1038/s41586-020-03073-y>.
33. Lee, S.A., Miller, J.F., Watrous, A.J., Sperling, M.R., Sharan, A., Worrell, G.A., Berry, B.M., Aronson, J.P., Davis, K.A., Gross, R.E., et al. (2018). Electrophysiological signatures of spatial boundaries in the human subiculum. *J. Neurosci.* 38, 3265–3272. <https://doi.org/10.1523/JNEUROSCI.3216-17.2018>.
34. Chen, D., Kunz, L., Wang, W., Zhang, H., Wang, W.X., Schulze-Bonhage, A., Reinacher, P.C., Zhou, W., Liang, S., Axmacher, N., and Wang, L. (2018). Hexadirectional modulation of theta power in human entorhinal cortex during spatial navigation. *Curr. Biol.* 28, 3310–3315.e4. <https://doi.org/10.1016/j.cub.2018.08.029>.
35. Chen, D., Kunz, L., Lv, P., Zhang, H., Zhou, W., Liang, S., Axmacher, N., and Wang, L. (2021). Theta oscillations coordinate grid-like representations between ventromedial prefrontal and entorhinal cortex. *Sci. Adv.* 7, eabj0200. <https://doi.org/10.1126/sciadv.abj0200>.
36. Doeller, C.F., Barry, C., and Burgess, N. (2010). Evidence for grid cells in a human memory network. *Nature* 463, 657–661. <https://doi.org/10.1038/nature08704>.
37. Miller, K.J., Sorensen, L.B., Ojemann, J.G., and den Nijs, M. (2009). Power-law scaling in the brain surface electric potential. *PLoS Comp. Biol.* 5, e1000609. <https://doi.org/10.1371/journal.pcbi.1000609>.
38. Sherrill, K.R., Erdem, U.M., Ross, R.S., Brown, T.I., Hasselmo, M.E., and Stern, C.E. (2013). Hippocampus and retrosplenial cortex combine path integration signals for successful navigation. *J. Neurosci.* 33, 19304–19313.
39. Viard, A., Doeller, C.F., Hartley, T., Bird, C.M., and Burgess, N. (2011). Anterior hippocampus and goal-directed spatial decision making. *J. Neurosci.* 31, 4613–4621.
40. Patai, E.Z., Javadi, A.-H., Ozubko, J.D., O'Callaghan, A., Ji, S., Robin, J., Grady, C., Winocur, G., Rosenbaum, R.S., and Moscovitch, M. (2019). Hippocampal and retrosplenial goal distance coding after long-term consolidation of a real-world environment. *Cereb. Cortex* 29, 2748–2758.
41. Slone, E., Burles, F., and Iaria, G. (2016). Environmental layout complexity affects neural activity during navigation in humans. *Eur. J. Neurosci.* 43, 1146–1155. <https://doi.org/10.1111/ejn.13218>.

42. Kunz, L., Maidenbaum, S., Chen, D., Wang, L., Jacobs, J., and Axmacher, N. (2019). Mesoscopic neural representations in spatial navigation. *Trends Cogn. Sci.* 23, 615–630.
43. Ekstrom, A. (2010). How and when the fMRI BOLD signal relates to underlying neural activity: the danger in dissociation. *Brain Res. Rev.* 62, 233–244.
44. Spiers, H.J., Olafsdottir, H.F., and Lever, C. (2018). Hippocampal CA1 activity correlated with the distance to the goal and navigation performance. *Hippocampus* 28, 644–658. <https://doi.org/10.1002/hipo.22813>.
45. Wang, Y., Romani, S., Lustig, B., Leonardo, A., and Pastalkova, E. (2015). Theta sequences are essential for internally generated hippocampal firing fields. *Nat. Neurosci.* 18, 282–288. <https://doi.org/10.1038/nn.3904>.
46. Iglói, K., Doeller, C.F., Berthoz, A., Rondi-Reig, L., and Burgess, N. (2010). Lateralized human hippocampal activity predicts navigation based on sequence or place memory. *Proc. Natl. Acad. Sci. USA* 107, 14466–14471.
47. Lyttle, D., Gereke, B., Lin, K.K., and Fellous, J.M. (2013). Spatial scale and place field stability in a grid-to-place cell model of the dorsoventral axis of the hippocampus. *Hippocampus* 23, 729–744. <https://doi.org/10.1002/hipo.22132>.
48. Spiers, H.J., and Maguire, E.A. (2006). Thoughts, behaviour, and brain dynamics during navigation in the real world. *Neuroimage* 31, 1826–1840.
49. Patai, E.Z., and Spiers, H.J. (2021). The versatile wayfinder: prefrontal contributions to spatial navigation. *Trends Cogn. Sci.* 25, 520–533.
50. Donoghue, T., Haller, M., Peterson, E.J., Varma, P., Sebastian, P., Gao, R., Noto, T., Lara, A.H., Wallis, J.D., and Knight, R.T. (2020). Parameterizing neural power spectra into periodic and aperiodic components. *Nat. Neurosci.* 23, 1655–1665.
51. Doeller, C.F., King, J.A., and Burgess, N. (2008). Parallel striatal and hippocampal systems for landmarks and boundaries in spatial memory. *Proc. Natl. Acad. Sci. USA* 105, 5915–5920. <https://doi.org/10.1073/pnas.0801489105>.
52. Kunz, L., Wang, L., Lachner-Piza, D., Zhang, H., Brandt, A., Dümpelmann, M., Reinacher, P.C., Coenen, V.A., Chen, D., and Wang, W.-X. (2019). Hippocampal theta phases organize the reactivation of large-scale electrophysiological representations during goal-directed navigation. *Sci. Adv.* 5, eaav8192.
53. M Aghajan, Z., Schuette, P., Fields, T.A., Tran, M.E., Siddiqui, S.M., Hasulak, N.R., Tcheng, T.K., Eliashiv, D., Mankin, E.A., Stern, J., et al. (2017). Theta Oscillations in the Human Medial Temporal Lobe during Real-World Ambulatory Movement. *Curr. Biol.* 27, 3743–3751.e3. <https://doi.org/10.1016/j.cub.2017.10.062>.
54. Gelinás, J.N., Khodagholy, D., Thesen, T., Devinsky, O., and Buzsáki, G. (2016). Interictal epileptiform discharges induce hippocampal-cortical coupling in temporal lobe epilepsy. *Nat. Med.* 22, 641–648. <https://doi.org/10.1038/nm.4084>.
55. Fischl, B. (2012). FreeSurfer. *Neuroimage* 62, 774–781. <https://doi.org/10.1016/j.neuroimage.2012.01.021>.
56. Jenkinson, M., Beckmann, C.F., Behrens, T.E.J., Woolrich, M.W., and Smith, S.M. (2012). FSL. *NeuroImage* 62, 782–790. <https://doi.org/10.1016/j.neuroimage.2011.09.015>.
57. Qin, C., Tan, Z., Pan, Y., Li, Y., Wang, L., Ren, L., Zhou, W., and Wang, L. (2017). Automatic and precise localization and cortical labeling of subdural and depth intracranial electrodes. *Front. Neuroinform.* 11, 10. <https://doi.org/10.3389/fninf.2017.00010>.
58. Martínez-Huertas, J., Olmos, R., and Ferrer, E. (2021). Model selection and model averaging for mixed-effects models with crossed random effects for subjects and items. *Multivariate Behav. Res.* 57, 603–619. <https://doi.org/10.1080/00273171.2021.1889946>.

STAR★METHODS

KEY RESOURCES TABLE

REAGENT or RESOURCE	SOURCE	IDENTIFIER
Software and algorithms		
MATLAB 2022	The MathWorks, Natick, MA, USA	https://ww2.mathworks.cn/products/matlab.html
Freesurfer v6.0.0	Athinoula A. Martinos Center for Biomedical Imaging at Massachusetts General Hospital	surfer.nmr.mgh.harvard.edu/
FSL	FMRI, Oxford, UK	https://fsl.fmrib.ox.ac.uk/fsl/fslwiki/FSL
PyLocator	Thorsten Kranz	http://pylocator.thorstenkranz.de/
FOOOF	Donoghue et al. ⁵⁰	https://fooof-tools.github.io/fooof/

RESOURCE AVAILABILITY

Lead contact

Further information and requests for resources should be directed to and will be fulfilled by the lead contact, Liang Wang (lwang@psych.ac.cn).

Materials availability

This study did not generate any unique materials.

Data and code availability

- All behavioral and neural data used in this study are available from the [lead contact](#) upon request (due to the size of the dataset).
- All custom MATLAB scripts related to this paper are available on GitHub: <https://github.com/chendong567/goaldistance> and are publicly available as of the date of publication.
- Any additional information required to reanalyze the data reported in this paper is available from the [lead contact](#) upon request.

EXPERIMENTAL MODEL AND STUDY PARTICIPANT DETAILS

Nineteen patients undergoing treatment for pharmaco-resistant epilepsy who implanted with hippocampal electrodes were recruited in the current study. All patients were implanted with stereoelectroencephalography (SEEG) depth electrodes for localization of epileptogenic regions. Implantation sites were based on clinical considerations. Four patients who have less than 12 good trials were excluded due to their inability to learn the navigation task. The information of the remaining 15 subjects is shown in [Table 1](#), of which six patients had contacts in the right hippocampus, six patients had contacts in the left hippocampus, and three patients had contacts in the bilateral hippocampus (4 females; age, 26.33 ± 5.08 years; see further details in [Table 1](#)). The study was approved by the local institutional review board, and written informed consent was obtained from all participants.

METHOD DETAILS

Experiment task

The object-location memory task was programmed using Unreal Engine 2 (Epic Games), and participants navigated freely in a circular virtual arena from a first-person perspective.^{34,35,51} The virtual environment consisted of a grassy plane with a diameter of about 9500 virtual units (vu) bounded by a cylindrical cliff and several distal orientation cues: two mountains, a sun, and some clouds. Participants used the arrow keys on the laptop keyboard (left, right, and forward arrows) to control their movement and the spacebar key to indicate their response. Keeping pressing the forward arrow resulted in an acceleration until maximum speed was reached.

The task started with an initial learning phase. The participants were first placed in the center of the maze and one object appeared. Participants were instructed to pick up the object. Whenever the object was picked up, the next object can be appeared. Therefore, the starting point for the next object was the true position of the previous object. Participants then performed memory recall trials ([Figure 1A](#)). Each trial began with a presentation of the cued target object for 2 s. Next, participants freely navigated to the target ('retrieval' phase). After participants had made a button-press response at the assumed goal location, feedback was shown for 1.5 s, which differed depending on the drop error (i.e., the distance between the response location and the true goal location; [Figure 1B](#)) ('feedback' phase). Feedback ranged from strongly positive (green smiley face) to strongly negative (red frown face);

Figure 1C). Finally, the target object for that trial was presented in its correct location and participants collected the object from there, allowing for further learning ('re-encoding' phase). A fixation crosshair was shown for 3 to 5 s (randomly jittered) between trials. Behavioral data were continuously written to a logfile. Participants completed a variable number of trials depending on their compliance.

Intracranial EEG recordings and preprocessing

Intracranial EEG recordings were conducted in Chinese and German hospitals separately, see further detail in previous studies.^{34,35,52} IEEG data were acquired using a Compumedics system (Compumedics, Abbotsford, Victoria, Australia) at a sampling rate of 2000 Hz in Freiburg, a Nihon-Kohden system (Yuquan Hospital) and a Blackrock NeuroPort system (First Affiliated Hospital of PLA General Hospital) at a sampling rate of 2000 Hz or 1000 Hz in Beijing. All data were re-referenced to the nearest white-matter contact. The re-referenced signals were notch-filtered at 50 Hz and their harmonics to remove power line noise. Then we applied a detection procedure based on the statistical properties of signal envelope to identify epileptic discharges and other artifacts.^{34,35,53,54} Specifically, signals were detected as interictal epileptiform discharges when either of the following two criteria was met: (i) the envelope of the unfiltered signal was 4 SDs above its mean value; (ii) the envelope of the filtered signal (25–80 Hz) was 5 SDs above its mean value. All signals were also visually inspected for interictal spikes. Intervals with artifacts on each channel were excluded from further analyses.

Electrode localization

For participants from Beijing, post-implantation CT was co-registered onto the pre-implantation MRI using FreeSurfer Software Suite⁵⁵ (<https://surfer.nmr.mgh.harvard.edu/>) and FMRIB Software Library⁵⁶ (<https://fsl.fmrib.ox.ac.uk/>). The intracranial electrodes were localized using our custom toolbox.⁵⁷ Then all electrodes were mapped onto Montreal Neurological Institute (MNI) standard space for visualization. For participants from Germany, post-implantation MRI was co-registered onto the pre-implantation MRI using FMRIB Software Library. The post-implantation MRI was normalized to MNI space. The normalized post-implantation MRI was further visually inspected using PyLocator (<http://pylocator.thorstenkranz.de/>) to manually identify the electrode locations.

Data analysis

To analyze the spectral properties of the hippocampus signals, the preprocessed signals were convolved with six-cycle Morlet wavelets at 50 logarithmically spaced frequencies ranging from 2 to 150 Hz. The power values were log transformed and then z-scored according to the mean and standard deviation of the power during all movement periods. As in previous studies,^{34,35} fast movement epochs were defined as periods during retrieval phases with speed exceeding the fastest tercile of all movement speed. Spectral properties of the hippocampus during fast epochs in retrieval phases were extracted for further statistics.

To estimate whether and how neural oscillations were modulated by goal distances, the entire data were bandpass-filtered (2–5 Hz, 6–9 Hz, 10–16 Hz, 30–100 Hz, 70–150 Hz). Then, oscillatory power of each frequency band was extracted using a Hilbert transform. The power was then normalized as described above.

Analyses of goal distance modulation employed only the fastest tertile of movement periods in the retrieval phase, assuming that participants were more confident about the assumed goal location when they were traveling at high speed. Given the fact that goal distance representations depend on spatial memory, goal distance representations are supposedly not precise if subjects did not recall the target location successfully. Therefore, we split the trials into two groups depending on drop error: Trials with a drop error less than 1500 vu were treated as good trials (positive and neutral feedback, 41.09% of all trials), otherwise they were bad trials (negative feedback, 58.91% of all trials).³⁵ Goal distance modulation was calculated separately for good and bad trials. The amount of data in good and bad trials was not different ($t(14) = -0.127$, $p = 0.901$). Goal distance was defined as the Euclidean distance between the instantaneous location and the true goal location (Figure 1B), and then rescaled within the range between 0 and 1 over all trials, where a value of 0 represents a distance of zero from the goal and a value of 1 reflects the location furthest away from the goal.^{9,11} For each channel, we predicted the z-scored normalized power in each frequency band during fast epochs of the retrieval phase by the corresponding goal distance. Specifically, the z-scored power served as the dependent variable, while the corresponding rescaled goal distance served as the independent variable. The regression was performed using Matlab *fitglm.m* function as follow.

$$\text{Power} \sim 1 + \beta \cdot \text{Goal distance}$$

This resulted in one goal distance modulation (β) for each contact at each frequency band and trial category (good and bad trials).

Given that the traditional method was susceptible to neural oscillations, we calculated neuronal timescales (τ) using a new method specifically developed for intracranial recordings. In particular, we utilized the python FOOF toolbox⁵⁰ to parametrize the power spectrum for periodic (oscillation) and aperiodic (1/f like) components.

For periodic components, we detected local frequency peaks within the 4–12 Hz range in 40 contacts, and examined the relationship between those peaks and the longitudinal axis of the hippocampus.

For non-periodic components, theoretical modeling shows that after removing the oscillations, the autocorrelation function of the time series has the form of $e^{-\frac{t}{\tau}}$, and its Fourier transform has the form of the Lorentzian function: $\frac{A}{f^2 + f_{knee}^2}$, where f_{knee} corresponds to the point where the slope changes rapidly.^{26,37}

In FOOF toolbox, the aperiodic component L was modeled as follows:

$$L = b - \log(k + F^x)$$

where b is the offset, F is the predefined frequency band. x is the exponent and k is the ‘knee’ parameter. To avoid the influence of low-frequency oscillations in the data, we fit f_{knee} in the range of 12–150 Hz according to previous suggestions.³⁷ Non-zero k value suggests a bend in the aperiodic component, in which case the knee frequency f_{knee} can be inferred using the following formula:

$$f_{knee} = k^{1/x}$$

Finally, the timescale can be computed as:

$$\tau = \frac{1000}{2\pi f_{knee}}$$

We detected knee frequency in 42 contacts, and obtained the τ values from those contacts. It is worth noting that not all PSDs showed an apparent knee frequency.

QUANTIFICATION AND STATISTICAL ANALYSIS

All statistical tests were performed using linear mixed-effect (LME) models with the Matlab *fitlme.m* function. LME models are well suited to account for repeated measurements from one subject, because each subject was implanted with various number of electrode contacts.^{32,58} For power spectral properties and goal distance modulation, a random intercept model was used to examine whether the variable was significantly different from 0:

$$Y \sim 1 + (1|\text{Subject})$$

where the dependent variable Y was either goal distance modulation (β), oscillatory power, or a power contrast (good trials vs. bad trials). The term in the parentheses was the random effect of subjects (below the same).

In order to compare the theta power between left and right hippocampus, the LME model was defined as follows:

$$Y \sim 1 + X + (1|\text{Subject})$$

where the dependent variable Y was theta power, and the fixed effect X referred to brain hemisphere (left/right).

To examine whether either goal distance modulation or temporal hierarchy significantly varied along the hippocampal axis, the random intercept LME model was applied as follows:

$$Y \sim 1 + X + (1|\text{Subject})$$

where the dependent variable Y was goal distance modulation (β), neural timescale (τ) or theta peak, and the fixed effect X was the y coordinate of the hippocampal contacts in MNI space.